ESKİŞEHİR TEKNİK ÜNİVERSİTESİ BİLİM VE TEKNOLOJİ DERGİSİ B- TEORİK BİLİMLER

Eskişehir Technical University Journal of Science and Technology B- Theoritical Sciences

2018, Volume:6 - pp. 109-116, DOI: 10.20290/aubtdb.490007

4th INTERNATIONAL CONFERENCE ON EARTHQUAKE ENGINEERING AND SEISMOLOGY

DETECTION OF COLLAPSED BUILDING FROM UNMANNED AERIAL VEHICLE DATA WITH OBJECT BASED IMAGE CLASSIFICATION

Resul ÇÖMERT [1], Dilek KÜÇÜK MATCI [2], Uğur AVDAN [3]

[1] Department of Geomatics Engineering, Faculty of Engineering and Natural Sciences, Gümüşhane University, Gümüşhane, Türkiye

[2, 3] Instıtute of Earth and Space Sciences, Eskişehir Technical University, Eskişehir, Türkiye

ABSTRACT

Buildings are most affected the objects by earthquake disaster. Detection of collapsed buildings after an earthquake is important both for determining the current situation and quick response. Unmanned aerial vehicles that have evolved in recent years, can provide very high resolution images of the earth surface using camera systems attached to them. Information for the intended purpose can be obtained through the products produced from these images.

In this study, collapsed buildings were detected in the area where high-resolution images were obtained whit unmanned aerial vehicle in 2015 and 2014. Building detection process was made based on a scenario events. In this context, 2015 images were taken before the earthquake and 2014 images were taken after the earthquake. The images of both years were processed separately to produce the digital elevation model and orthophoto image of the study area. building of the study area were obtained by applying the object-based classification process to the generated data. 11 buildings which were available in the area in 2015 and not available in the area in 2014, were detected successfully comparison of building classes of two years.

Keywords: Collapsed Building, Object Based Classification, Remote Sensing, UAV

1. INTRODUCTION

During natural disasters, such as earthquakes, buildings are the most affected urban objects. The detection of collapsed buildings is important in order to expose the damage of the disaster and to mobilize the relevant institutions to mitigate the damage. The detection of building alterations is possible by using remote sensing technologies that provide up-to-date information. It is possible to determine the destroyed buildings by analyzing satellite images or aerial photographs obtained before and after the event which is known as change detection approach[1]. In addition to change detection approaches, object-based classification is another method used to derive buildings from high-resolution images [2].

The object-based classification approach is frequently encountered as a preferred method after the increase in the resolution of images obtained from remote sensing. In order to be able to identify the buildings destroyed from different date displays, it is first necessary to identify the buildings in these views separately. Based on object-based classification approach, several studies use high resolution satellite images [3, 4], LIDAR and satellite images [5]; From LIDAR data [6, 7]; high-resolution aerial photographs and numerical surface model [2].

In recent years, a new remote sensing platform, unmanned aerial vehicles (UAVs) have entered in our lives. These systems have a very useful detection platform feature, especially in small areas in terms of repeatability, low cost and high resolution data [8]. Very high resolution aerial photographs can be obtained with the UAV systems. Orthophoto, Digital Surface Modeling (DSM) and Digital Terrain Modeling (DTM) can be produced by processing the obtained aerial photographs. The spectral

*Corresponding Author: resulcomert@gmail.com
Received: 09.05.2018 Accepted:29.06.2018

information of the generated orthophoto, features of the DSM and DTM data can be used for height information building inference studies.

In this study, the availability scenario of an Orthophoto, DSM and DTM data generated from UAV data was examined through an event in the detection of destroyed buildings. Within this scope, the products produced from the data obtained from 2014 and 2015 belonging to Anadolu University Yunus Emre campus were used. In the scenario case, the products belonging to the year 2015 were accepted as the data before the earthquake and after the earthquake of the year 2014. The object-based classification method was applied to the data sets and the buildings in the field were semi-automated extracted. Removed buildings are subject to registration process and the 11 buildings that did not exist in 2014 but were resent in 2015 have been successfully detected.

2. STUDY AREA AND DATA SET

In this study, Anadolu University, Yunus Emre Campus was chosen as the study area. An aerial photograph of this area was carried out on August 31, 2014 and September 8, 2015 by the UAV system. Sensefly eBee unmanned aerial vehicle was used for image acquisition. This is a system that is manually launched and automatically landed on the body. Depending on the flight height, the images of the ground sample distance between 2 cm and 30 cm can be obtained with the visible RGB camera system attached to the UAV system.

The images of the study area were obtained with a single flight every two years. Flight operations were carried out at a height of approximately 160 meters, allowing photographs to be taken at 75% lateral and horizontal overlap. Ground Control Points (GCP) were placed in the pre-flight area every two years to ensure the positional accuracy of the produced data. Coordinate values of the control points were measured by the geodetic GNSS receiver. The resulting images were processed in Pix4D software to produce orthophoto images, DSM and DTM products in the field. Figure 1 shows orthophoto images for 2014 and 2015 as well as DSM and DTM data for 2014.

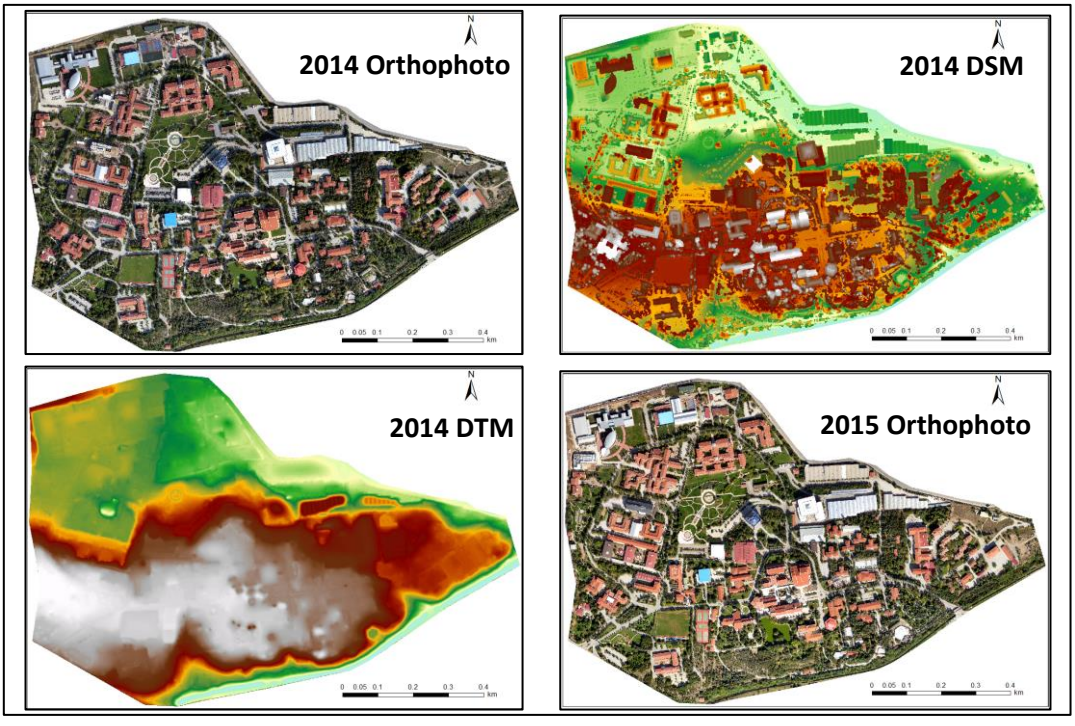

Figure 1. Orthophoto, DSM and DTM data produced for 2014 and orthophoto images for 2015 and 2014.

When the buildings in the study area are examined, it is seen that there are buildings with different height, shape and different roof colors. The data for the year 2015 were accepted as pre-event data and the data for the year 2014 were accepted as post – event data.

3. METHOD

An object-based classification approach has been used to extract buildings from the data that belongs to different years. Object-based classification is a classification method that includes spectral, shape, textural, geometric and contextual information in high resolution images. This method generally consists of image segmentation and classification stages. In this method, similar pixels are first grouped according to the condition of ensuring a certain homogeneity criterion, and image objects to be used in the classification process are formed. This is the segmentation phase of the method. After the segmentation process, rule sets for classification are formed in order to extract the desired detail from the image. Homogeneous object groups are assigned to classes according to these rule sets (Jiang et al., 2008).

Image segmentation process is the first step of object-based classification method. Image segmentation is generally performed in two different ways namely top-down and bottom-up. It is aimed to create smaller image objects from the big image in the top-down segmentation process. Chessboard segmentation, quadtree-based segmentation, and multi-threshold segmentation are the examples of this segmentation method.

Bottom – up segmentation methods try to obtain larger image objects by starting from the small image object level or pixel level, contrary to the top – down segmentation methods. The examples of such methods are spectral difference segmentation and multi-resolution image segmentation.

In the rule-based classification process applied after the segmentation process, rule sets are created according to the properties of the selected input layers. The spectral values of the bands used as inputs in the generation of the rule sets, the band indices generated from these bands, and the geometric properties of the image objects are utilized. In this phase, a threshold value is usually set for the selected features, and it is ensured that the image objects providing the prescribed rule are assigned to the corresponding class.

In the scope of the study, the process used to determine building changes consists of 4 steps (Figure 2). The object-based classification applied in the study was performed in Ecognition Developer 9 software. The orthophoto, DSM and DTM data of both halves were transferred to the software, in addition, the difference maps between the DSM and DTM, the slope of DSM, edge extraction filter were generated.

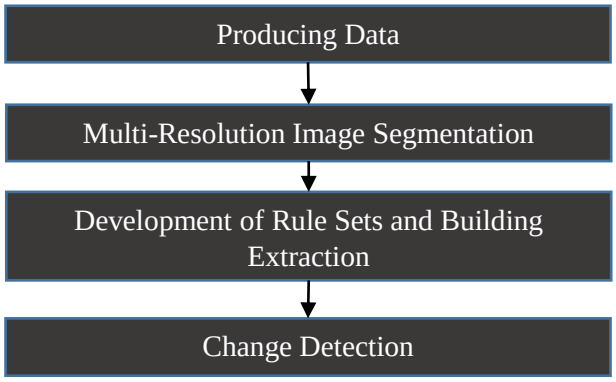

Figure 2. Process steps applied during change detection analysis

The image segmentation phase has been passed after the data that is to be used in practice has been generated. Multi-resolution segmentation method is applied as segmentation process, in which blue, green, red bands of the orthophoto image and edge filtering map are used as inputs. In order to create image segments that are used in classification with multi-resolution segmentation, the scale factor, shape and compactness parameters must be determined by the user. As a result of the experiments, the appropriate scale factor for the data set was obtained as 35, shape parameter 0.3 and compactness parameter 0.5. Figure 3 shows the image objects obtained as a result of the segmentation process.

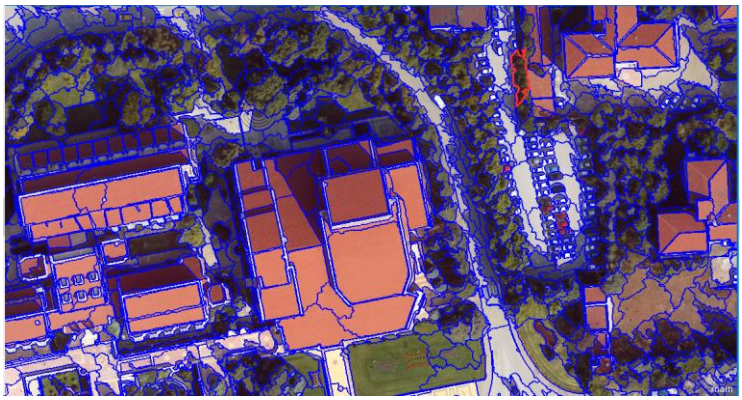

Figure 3. Image objects

After the segmentation process, the classification stage was performed. Rule sets have been developed for the classification. In the development of the rule sets, the difference between DSM and DTM, the geometric properties of the image object, the brightness value, the slope and the standard deviations of the layers have been utilized from the band indices produced from orthophoto bands. The band indices used in the study are given in Table 1.

Table 1. Band indices used in building extraction

Band Indice	Formula	Reference
Average Band Ratio (ABR)	$\frac{Red + Blue + Green}{3}$	Applied in this study.
Red, Green Band Track (R-G)	$Red - Green$	Applied in this study.
(EGI) Excess green index	$(2x\ Green) - Blue - Red$	[9]
(GLI) Green Leaf Index	$\frac{(2x\ Green) - Blue - Red}{(2x\ Green) + Blue + Red}$	[10]
(TGI) Triangular Greenery Index	$Green - (0.39xRed - 0.69xBlue)$	[10]
Green Band Ratio (GBR)	$\frac{Green}{Blue + Green + Red}$	[11]
Blue Band Ratio (BBR)	$\frac{Blue}{Blue + Green + Red}$	Applied in this study.
Normalized aquatic plant index (NRAVI)	$\frac{Green - Red}{Green + Red}$	[12]
Visible Region Atmospheric Endurance Index (VARI)	$\frac{Green - Red}{Blue + Green + Red}$	[13]
(ER) Excess red vegetation index	$(1.4\ x\ Red) - Green$	[14]

There are buildings with red, brown, green, blue and white roofs in the study area. These buildings were prepared separately according to the developed set of rules. Table 2 shows the parameters and

threshold values of the rule sets developed in the year 2014 and 2015 when the buildings in the district were removed. In the classification phase, the ground objects and the shaded areas are classified first, then the buildings with different roof colors are classified. After the classification process, the buildings of different roof colors are combined into a single class. Areas such as shadows and chimney vacancies in interior areas of building boundaries have been assigned to the building class, by taking into account the border neighborhoods of image segments. In addition, no area buildings and small areas like buildings are removed from the building class considering the pixel numbers.

Table 2. Parameters used in rule sets developed for classification

2014		2015	
Class	**Parameter**	**Class**	**Parameter**
Ground Object	$DSM - DTM \leq 3$	Ground Object	$DSM - DTM \leq 3$
Shadow	$ABR < 60$	Shadow	$ABR < 110$
Red Roof	$EGI < -2$	Red Roof	$0 \leq Edge\ Filter \leq 0.1$
	$-52 \leq TGI \leq -10$		$NRAVI < 0.07$
Brown Roof	$-56 \leq EGI \leq -2$	Brown Roof	$156 \leq Brightness \leq 190$
	$0.011 \leq Edge\ Filter \leq 0.09$		$-56 \leq EGI \leq 11$
	$1 \leq Slope \leq 6.5$		$Slope < 10$
	$TGI < 0$		$-30 \leq TGI \leq 2$
	$-0.09 \leq VARI \leq -0.002$		$-0.3 \leq VARI \leq -0.03$
			$20 \leq R\text{-}G \leq 100$
Blue Roof	$BBR \geq 0.42$	Blue Roof	$-160 \leq R\text{-}G \leq -25$
			$0 \leq VARI \leq 0.16$
Green Roof	$100 \leq ABR \leq 195$	Green Roof	$110 \leq ABR \leq 210$
	$0.1 \leq Slope \leq 5$		$0.1 \leq Slope \leq 6$
	$0.02 \leq nEGI \leq 0.07$		$0.02 \leq nEGI \leq 0.08$
	$0.02 \leq VARI \leq 0.07$		$NRAVI > 0$
White Roof	$-62 \leq ER \leq 102$	White Roof	$250 \leq Brightness \leq 325$
	$0.32 \leq GBR \leq 0.36$		$-62 \leq ER \leq 105$
	$0 \leq Slope\ Standard\ deviation \leq 10$		$0.32 \leq GBR \leq 0.36$
			$0.6 \leq Slope \leq 20$
	$TGI < -10$		$-25 \leq TGI \leq -5$

The buildings which are produced as a result of the classification process are presented in Figure 4.

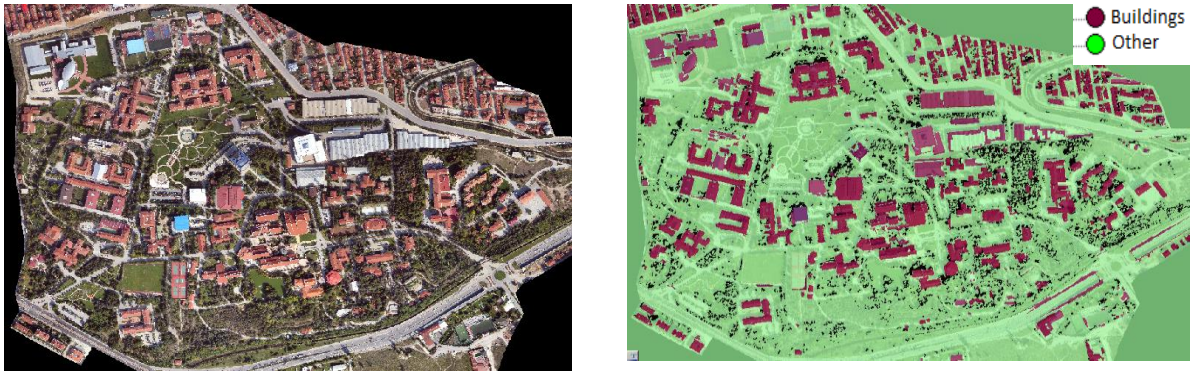

Figure 4. Classification operation result map for 2014.

After the classification and merging processes, the comparison process of the two years' buildings is started. The buildings in Ecognition software are exported in vector format. ArcGIS software has been used by buildings to identify building changes between 2015 and 2014. The data in the vector format of both years have been converted to raster form. Each building in the raster format is assigned a value of 1 for the year 2015 and 2 for the year 2014. Then these data sets were collected and different

buildings were detected. Areas with aggregate raster totaling 3 in the aggregate are 2015 and 2014 and those with a total area of raster 1 are in the area in 2015. The areas without raster in 2014 and the areas with raster total 2 are not in the area in 2015, (Figure 5). In this study, pre-event image 2015, post-event image 2014 are accepted, so the areas with raster value 1 are demolished buildings.

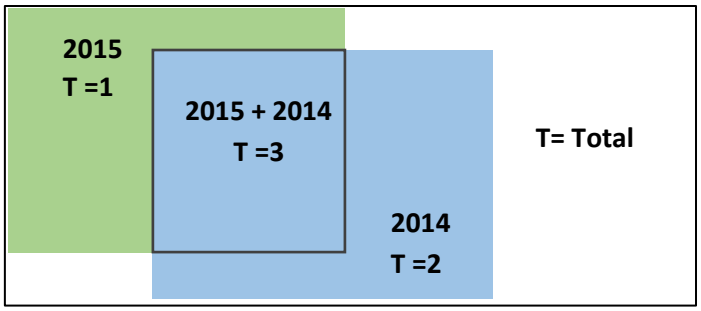

Figure 5. The method used to find building differences

The result of the comparison is shown in Figure 6. According to the results, there are 11 different structures in the area. These changes have been successfully detected. However, some shadow areas and some areas similar to the building roof colors have been removed as building areas during the building extraction process.

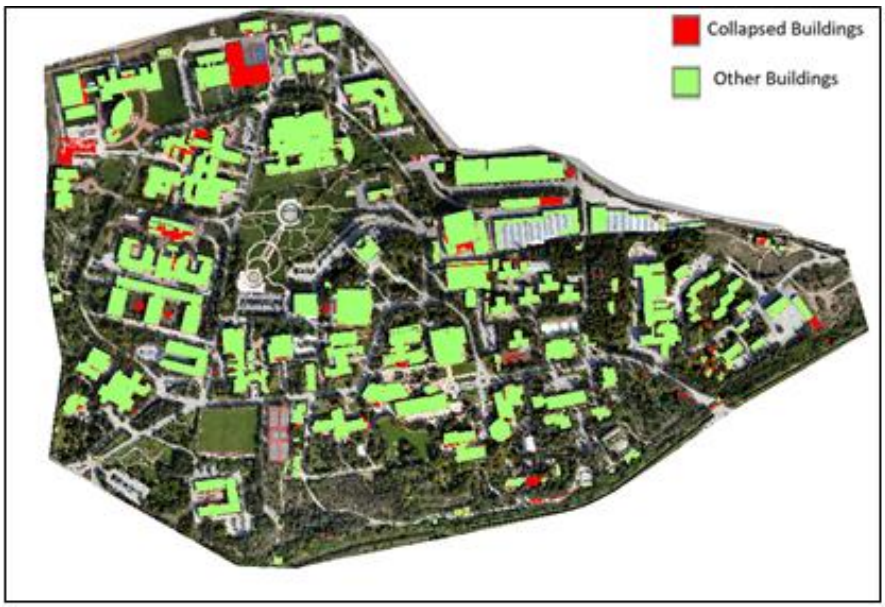

Figure 6. Buildings collapsed, according to the comparison scenario

4. RESULTS AND DISCUSSIONS

Within the scope of the study, the building extraction process was performed with the object-based classification approach from the data produced from the 2015 and 2014 UAV images. Rule sets for the year 2014 have been developed primarily for building extraction. It was then applied to the 2015 data set without any changes to the rule sets developed for 2014. As a result of this implementation, the parameters and threshold values used in the rule set created for the 2014 data did not work successfully in 2015. Therefore, a separate rule set has been defined for the 2015 data set. The reason for not operating the same set of rules in the data sets is considered to be related to the time of acquisition of the data with UAV and the whether condition at the time.

With the developed rule sets, it was seen that while the buildings belonging to both sides were inferred, they were excavated as buildings in different objects which are not buildings. In the study, the areas with the DSM and DTM difference smaller than 3 meters were accepted as the ground object. There are similar places in the upper area. In these areas, some high areas similar to the colors of the canopy and the roof were extracted as buildings (Figure 7a). In the same way, it was observed that truck-type high-stall vehicles with a height difference of more than 3 meters were extracted as buildings (Figure 7b). In addition to this, the location is not clearly defined in the software where the data is produced, especially when the DTM is generated in the areas covered with trees. It has therefore been observed that a complete nude terrain model cannot be produced in such areas. In these buildings, the DSM and DTM difference is smaller than 3 meters, and some parts of these buildings are classified as ground objects (Figure 7c).

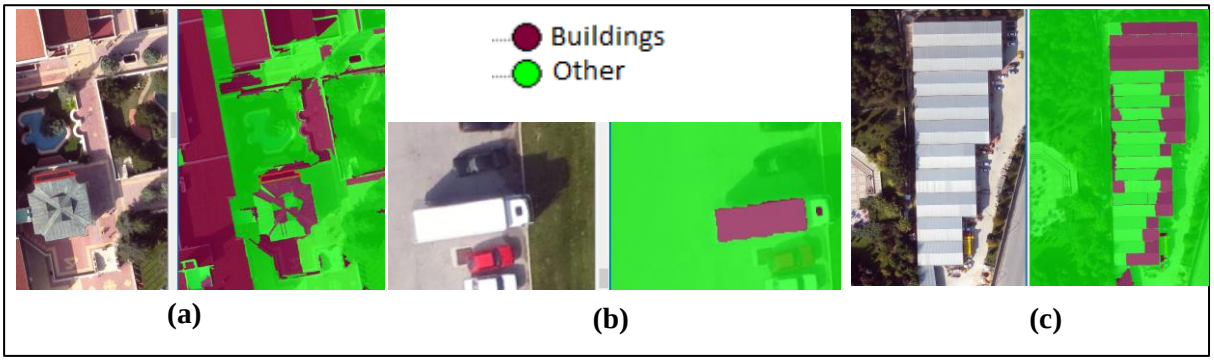

Figure 7. (a): areas such as overpasses and similar color to the building roof; **(b):** a high-stowed vehicle removed as a building; **(c):** The building removed as a ground object from the error in the DTM data.

5. CONCLUSION

In this study, the collapsed buildings were determined by object-based classification approach by using scenario data of different dates on an event. The scenario is considered to be the case for the year 2015 and the case for the year 2014 before the event. A separate set of rules has been developed for the determination of buildings for two years. With the developed rule sets, buildings of different years have been extracted from the image. By comparison of the buildings extracted, 11 buildings considered to have been destroyed on the scene due to the scenario event have been identified. Beside the buildings found, the datasets were seen as the buildings in the non-building objects. Errors in the shadow, DTM production, and objects resembling the building skylights were the main sources of error in the scope of the study. Future work will need to be carried out in order to overcome the defects caused by building inferences.

REFERENCES

[1] Sumer E and Turker M. Building damage detection from post-earthquake aerial images using watershed segmentation in Golcuk, Turkey. International Society for Photogrammetry and Remote Sensing ISPRS, 2004: p. 642-647.

[2] Jiang N, et al., Object-oriented buinding extraction by DSM and very high-resolution orthoimages. The International Archives of the Photogrammetry, Remote Sensing and Spatial Information Sciences, 2008. 37: p. 441-446.

[3] Yano Y, et al. Building damage detection of the 2003 Bam, Iran earthquake using QuickBird images. in Proceedings of the 25th Asian Conference on Remote Sensing. 2004. Citeseer.

[4] Safarlou F, Change Detectıon of Buildings from High Resolution Satellite Imagery And Existing Map Data Using Object Based Classification. 2015.

[5] Teo T-A and L.-C. Chen. Object-based building detection from LiDAR data and high resolution satellite imagery. in Proceedings of the 25th Asian Conference on Remote Sensing. 2004.

[6] Rutzinger M, et al. Object-based building detection based on airborne laser scanning data within GRASS GIS environment. in Proceedings of UDMS. 2006.

[7] Miliaresis G and N. Kokkas, Segmentation and object-based classification for the extraction of the building class from LIDAR DEMs. Computers & Geosciences, 2007. 33(8): p. 1076-1087.

[8] Hunt ER, et al., Acquisition of NIR-green-blue digital photographs from unmanned aircraft for crop monitoring. Remote Sensing, 2010. 2(1): p. 290-305.

[9] Woebbecke DM, et al., Color indices for weed identification under various soil, residue, and lighting conditions. Transactions of the ASAE, 1995. 38(1): p. 259-269.

[10] Hunt Jr ER, et al., A visible band index for remote sensing leaf chlorophyll content at the canopy scale. International Journal of Applied Earth Observation and Geoinformation, 2013. 21: p. 103-112.

[11] Baatz M, et al., eCognition user guide. Definiens Imaging GmbH, Munich, Germany, 2004.

[12] Tucker CJ, Red and photographic infrared linear combinations for monitoring vegetation. Remote sensing of Environment, 1979. 8(2): p. 127-150.

[13] Gitelson AA, et al., Novel algorithms for remote estimation of vegetation fraction. Remote sensing of Environment, 2002. 80(1): p. 76-87.

[14] Mao W, Wang Y and WangY. Real-time detection of between-row weeds using machine vision. in 2003 ASAE Annual Meeting, 2003. American Society of Agricultural and Biological Engineers.